Investigating the effect of positional isomerism on the assembly of zirconium phosphonates based on tritopic linkers

Received 00th January 20xx,
Accepted 00th January 20xx

DOI: 10.1039/x0xx00000x

Marco Taddei,[a,*] Stephen J. I. Shearan,[a] Anna Donnadio,[b] Mario Casciola,[c] Riccardo Vivani,[b] Ferdinando Costantino[c]

We report on the use of a novel tritopic phosphonic linker, 2,4,6-tris[3-(phosphonomethyl)phenyl]-1,3,5-triazine, for the synthesis of a layered zirconium phosphonate, named UPG-2. Comparison with the structure of the permanently porous UPG-1, based on the related linker 2,4,6-tris[4-(phosphonomethyl)phenyl]-1,3,5-triazine, reveals that positional isomerism disrupts the porous architecture in UPG-2 by preventing the formation of infinitely extended chains connected through Zr-O-P-O-Zr bonds. The presence of free, acidic P-OH groups and an extended network of hydrogen bonds makes UPG-2 a good proton conductor, reaching values as high as 5.7x10^{-4} S cm^{-1}.

The quest for porous metal phosphonates is a niche research area that was first explored in the early 90s[1] and has recently gained renewed momentum,[2] thanks to some novel synthetic approaches that have granted access to ordered and porous compounds. Use of phosphonate monoester linkers, which feature similar coordination geometry to carboxylates, has been explored in a systematic fashion, leading to several microporous compounds.[3-6] Post-synthetic hydrolysis of the phosphonate ester groups has also been demonstrated, with benefits to the CO_2 affinity of the framework.[7, 8]An alternative approach based on a similar rationale involves phosphinates as carboxylic acid analogues, affording a series of Fe-based compounds with isoreticular structures and high porosity.[9] One peculiar and intriguing feature of these materials is that functionalization of the framework can be accomplished by tuning the size and nature of the pending group attached to the P atom. Introduction of ancillary ligands, e.g. bipyridines or dicarboxylates, which can act as additional bridging units connecting different inorganic struts, has also been successful in generating porous materials based on either phosphonic or phosphinic linkers.[10-13] Shifting the focus to the reaction medium, ionic liquids have recently been found to promote the formation of secondary building units, similar to those observed in carboxylate-based metal-organic frameworks (MOFs), yielding single crystals of three new zirconium phosphonates with open framework structures.[14] The use of linkers having specific geometrical features, not compatible with the formation of the dense inorganic layers typical of metal phosphonates, is another strategy of election for inducing porosity in this family of materials.[15-17] Several reports have appeared over the last few years, involving tritopic,[18-22] tetrahedral[14, 23-25] and tetratopic square linkers,[26-28] which prove that tuning the geometry and symmetry of the linker is indeed an effective way to access open framework architectures, reaching surface areas above 1000 m^2 g^{-1}. Besides porosity, the most striking characteristic of these phosphonate-based MOFs is their exceptional chemical stability, which often exceeds that of the most stable classical carboxylate-based counterparts. This can be attributed to the strong affinity of the phosphonic group for metal ions, which makes metal phosphonates very insoluble and resistant to hydrolysis, even in aggressive conditions.[29, 30] According to the hard and soft acids and bases (HSAB) theory,[31] combination of hard acids, such as Zr^{4+}, Ti^{4+}, Al^{3+}, Cr^{3+}, and hard oxygenated bases, such as carboxylate or phosphonate groups, leads to formation of strong metal-oxygen bonds.[32] The higher stability of metal phosphonates derives from the higher charge and the increased number of donor atoms of the -PO_3H_2 group.[29]

We recently reported on the synthesis of the first crystalline and microporous zirconium phosphonate, UPG-1,[19] which is based on the 2,4,6-tris[4-(phosphonomethyl)phenyl]-1,3,5-triazine linker (hereafter H_6*p*ttbmp, scheme 1). UPG-1 features two types of monodimensional channels with diameter of about 5 Å and 10 Å and is permanently porous, with a BET surface area of 410 m^2 g^{-1} and a pore volume of 0.2 cm^3 g^{-1} (Figure S1). In an effort to gain deeper understanding of the structure directing function of the linker, we have focused on the influence of positional isomerism on the assembly of the crystal structure. To this purpose, we have prepared the novel 2,4,6-tris[3-(phosphonomethyl)phenyl]-1,3,5-triazine linker (hereafter

[a] *Energy Safety Research Institute, Swansea University, Fabian Way, Swansea, SA1 8EN, United Kingdom. Email: marco.taddei@swansea.ac.uk*
[b] *Dipartimento di Scienze Farmaceutiche, University of Perugia, Via del Liceo 1, 06123 Perugia, Italy*
[c] *Dipartimento di Chimica Biologia e Biotecnologia, University of Perugia, Via Elce di Sotto 8, 06123 Perugia, Italy*

Electronic Supplementary Information (ESI) available: [Synthetic procedures; organic compounds characterisation (^{1}H NMR, ^{13}C NMR, HSQC, MS, FTIR); structure solution and refinement details; additional structural figures; additional PXRD patterns]. See DOI: 10.1039/x0xx00000x

H_6*m*tttbmp, scheme 1), where the phosphonomethyl moiety is in *meta* position with respect to the central triazine core, rather than in *para* position as in H_6*p*tttbmp.

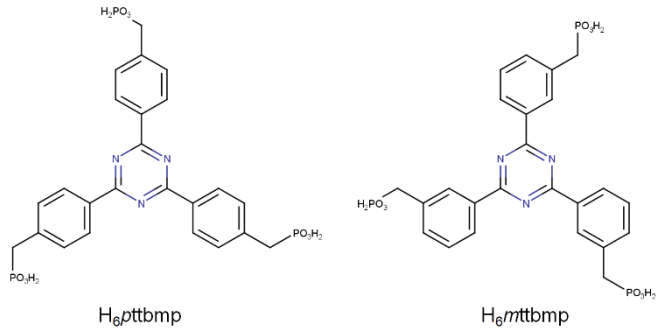

Scheme 1. Molecular formulae of the H_6*p*tttbmp and H_6*m*tttbmp linkers.

H_6*m*tttbmp was synthesised following a very similar three-step route to that previously developed for H_6*p*tttbmp[19] (see ESI for details and full characterisation of intermediate and final products, Figures S2-15). H_6*m*tttbmp was employed as a linker for the synthesis of a new microcrystalline zirconium phosphonate, named UPG-2, whose structure was determined and refined using powder X-ray diffraction (PXRD) data (see ESI for details on structure solution and refinement, Table S1, Figure S16). The crystal structure of UPG-2 is shown in Figure 1.

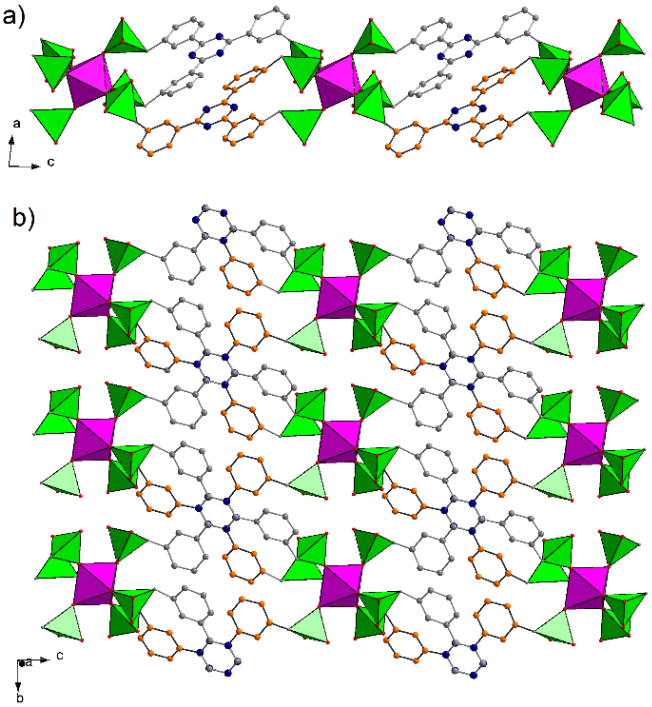

Figure 1. View of the crystal structure of a single layer of UPG-2 along the *b* axis (a) and perpendicular to the *bc* plane (b). The carbon atoms belonging to the linker molecule lying lower along the *a* axis are coloured in orange for the sake of clarity. Colour code: Zr, pink; P, green; N, blue; O, red; C, grey and orange.

UPG-2 crystallizes in the triclinic space group *P*-1, with lattice parameters a = 8.8147(4) Å, b = 9.6066(5) Å, c = 16.338(1) Å, α = 88.426(4) °, β = 83.914(4) °, γ = 85.607(4) °. The asymmetric unit consists of one Zr atom sitting on an inversion centre (special position with multiplicity = 1), one H_4*m*tttbmp^{2-} fragment and two water molecules (each with occupancy of 0.75). The Zr atom is octahedrally coordinated by six oxygen atoms belonging to six different phosphonate groups (three of which are crystallographically independent and three generated by symmetry). Each H_4*m*tttbmp^{2-} molecule is coordinated to three different Zr atoms through monodentate phosphonate groups. The resolution of PXRD data is not sufficient to locate hydrogen atoms, but, based on electroneutrality requirements, we can deduce that four of six P-O groups coordinated to Zr are negatively charged P-O$^-$, whereas two of them are neutral P=O. The presence of purely monodentate phosphonate groups is, to the best of our knowledge, observed here for the first time in any known zirconium phosphonate. This feature leads to lack of connection among ZrO_6 octahedra, which remain isolated from each other (the shortest Zr-Zr distance is 8.82 Å). The connection of isolated ZrO_6 octahedra and H_4*m*tttbmp^{2-} units gives rise to a layered structure, with layers about 9 Å thick lying in the *bc* plane. Each layer is connected to adjacent ones through a network of hydrogen bonds extending along the *b* axis that involves free P-O groups and two water molecules sitting in the interlayer space (Figure S17). Detailed views of the network of hydrogen bonds involving each phosphonate group and each water molecule are provided in Figures S18-22. In addition, a system of π-π stacking interactions extending along the *a* axis exists among the aromatic rings of H_4*m*tttbmp^{2-}, further contributing to efficient stacking of layers (Figure S23).

Given the similar linkers used for the synthesis of UPG-1 and UPG-2, detailed analysis and comparison of their structural features is in order. The two compounds were prepared in very similar reaction conditions: same temperature (80 °C), same Zr/linker/HF ratio (1:1:50), same concentration of metal and linker (0.018 M). Therefore, the differences in the resulting crystal structures can purely be attributed to the influence of the geometrical arrangement of the linkers. UPG-1 and UPG-2 display identical chemical composition (if extraframework water molecules are not considered), with the same Zr/linker ratio (1:2) and the linkers in the same protonation state (four protons of the original six are retained after reaction with the metal). Both linkers display a *cis-trans-trans* configuration of the phosphonate groups, with respect to the aromatic backbone, however the intramolecular P-P distances are significantly different: 13.0, 14.7 and 14.9 Å in UPG-1; 6.8, 12.4 and 13.8 Å in UPG-2 (Figure 2). This suggests that H_4*m*tttbmp^{2-} can adopt a more "compact" conformation than H_4*p*tttbmp^{2-}. A simple optimisation of the molecular structure of the linker H_6*m*tttbmp using the Merck molecular force field 94 (MMFF94),[33] as implemented in the software Avogadro,[34] reveals that the lowest energy configuration achievable displays two intramolecular hydrogen bonds between two phosphonic groups (Figure S24). The possible presence of these non-covalent interactions also in reaction conditions could explain why the linker H_6*m*tttbmp prefers the more compact conformation. As a result, the connectivity between the organic linkers and the metal atoms in UPG-1 and UPG-2 is remarkably different: both H_4*p*tttbmp^{2-} and H_4*m*tttbmp^{2-} are coordinated to

three Zr atoms, but the former linker displays one bidentate, one monodentate and one non-coordinated phosphonate group (Figure 2a), whereas the latter linker displays three monodentate phosphonate groups (Figure 2b). The presence of bidentate phosphonate groups in UPG-1 is ultimately crucial to afford connection of adjacent Zr atoms along the *c* axis direction and formation of infinite inorganic building units (IBUs) (Figure S25). These 1D IBUs are connected in the remaining two dimensions by the organic linkers, resulting in the formation of a 3D framework (Figure S1). As previously discussed, the lack of polydentate phosphonate groups prevents formation of extended IBUs in UPG-2 and, as a consequence, the structure cannot extend in the third dimension, giving rise to a 2D layered motif.

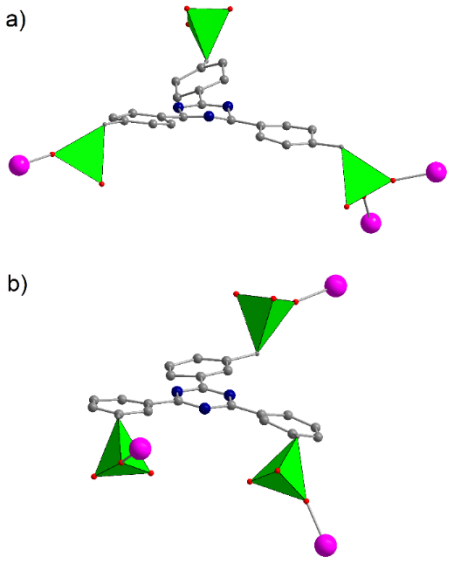

Figure 2. Linker conformation and connectivity in UPG-1 (a) and UPG-2 (b). Color code: Zr, pink; P, green; N, blue; O, red; C, gray.

The thermogravimetric curve of UPG-2, measured under air, is shown in Figure 3. The first weight loss, occurring at temperature lower than 130 °C, is attributed to the desorption of three water molecules per formula unit (calculated: 4.0%; observed: 4.0%). The compound is then stable until about 280 °C, when another 5.0% weight loss is observed. This loss could be due to some degree of condensation of the many free P-O groups present in the structure. Similar behaviour was observed for UPG-1.[19] Decomposition of the organic part of the structure takes place above 480 °C. The total weight loss at 1200 °C is 73.4%. Zirconium phosphonates with P/Zr ratio ≥ 2 usually thermally decompose to ZrP_2O_7.[35, 36] This product is also the only crystalline phase observed in the PXRD pattern of the decomposition residue of UPG-2 after TGA (Figure S26), allowing to calculate a weight loss of 80.0%, larger than the observed one. Since UPG-2 features an unusually high P/Zr ratio of 6, it is possible that part of the phosphonate groups is not completely decomposed at 1200 °C and a mixture of ZrP_2O_7 and other, amorphous phosphorus containing residues is formed.

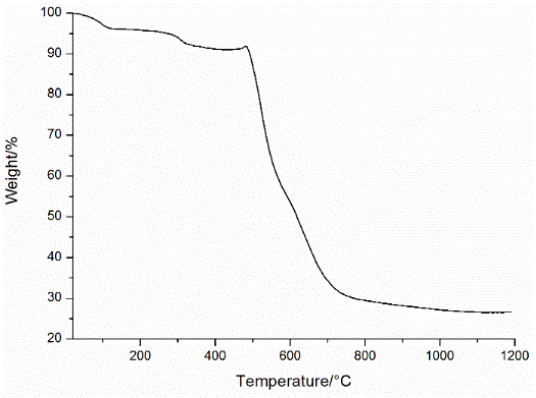

Figure 3.Thermogravimetric curve of UPG-2.

The proton conductivity of pellets of UPG-2 was measured at 100 °C, under controlled relative humidity (RH). Figure 4 shows that the conductivity increases by a factor of ca. 7, from 8.5×10^{-5} to 5.7×10^{-4} S cm^{-1}, with increasing RH from 40 to 95%. The value at 95% RH is in line with those previously observed for other Zr phosphonates.[37] To get insight into the physical origin of the proton transport, the hydration of UPG-2 was determined under the same conditions used to measure the conductivity. At 100 °C and 95% RH, UPG-2 takes up 6.2 water molecules per unit formula (about one water molecule per $–PO_3$ group), while 0.8 water molecules are lost after lowering RH to 40%. This loss appears to be too small to account for the large conductivity changes observed in this RH range. Therefore, it may be inferred that the pellet conductivity originates mainly from surface/intergrain proton transport and is affected by the hydration of the microcrystal surface, which is expected to be more susceptible than bulk hydration to RH changes. The excellent stability of UPG-2 in measurement conditions is proved by the PXRD pattern of the ground pellet, which is practically identical to that of the as synthesized material (Figure S27).

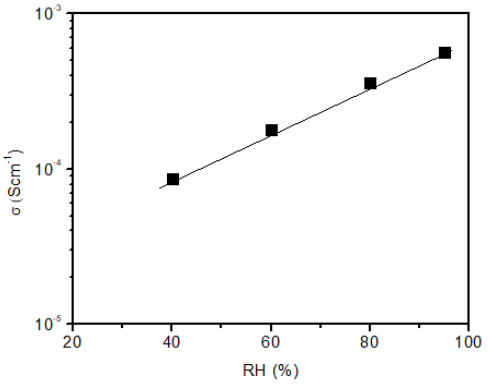

Figure 4. Proton conductivity of UPG-2 at 100 °C as a function of relative humidity.

Conclusions

In this work, we have investigated the effect of positional isomerism in tritopic phosphonic linkers on the assembly of the crystal structure of the relative Zr^{4+} derivatives. We found that

combination of Zr^{4+} and H_6*m*ttbmp, having -CH_2-PO_3H_2 groups in *meta* position with respect to the central triazine core, affords a compound with unprecedented 2D layered structure featuring isolated Zr octahedra (UPG-2), as opposed to the 3D open framework obtained when H_6*p*ttbmp, having -CH_2-PO_3H_2 groups in *para* position with respect to the central triazine core (UPG-1). The main structure-driving factor seems to be the ability of H_6*m*ttbmp to adopt a conformation where the intramolecular P-P distances are significantly shorter than in H_6*p*ttbmp, thus preventing formation of extended inorganic building units and development of the crystal structure in the third dimension. This is attributed to the presence of intramolecular hydrogen bonding interactions between phosphonic groups in the free linker. Thanks to the large number of hydrogen bonds involving phosphonic groups and water molecules, UPG-2 is a good proton conductor, reaching conductivity as high as $5.7x10^{-4}$ S cm^{-1} at 100 °C and 95% relative humidity. These results add to the existing body of knowledge concerning the crystal engineering of Zr phosphonates and can help in designing new phosphonic linkers with specific geometrical features to induce formation of structural arrangements with the desired dimensionality.

Conflicts of interest

There are no conflicts to declare.

Acknowledgement

The authors acknowledge the European Union's Horizon 2020 research and innovation programme under the Marie Skłodowska-Curie grant agreement No 663830 (M.T.) and the National Mass Spectrometry Facility (NMSF) at Swansea University.

Notes and references

1. K. Maeda, *Microporous Mesoporous Mater.*, 2004, **73**, 47-55.
2. S. J. I. Shearan, N. Stock, F. Emmerling, J. Demel, P. A. Wright, K. D. Demadis, M. Vassaki, F. Costantino, R. Vivani, S. Sallard, I. Ruiz Salcedo, A. Cabeza and M. Taddei, *Crystals*, 2019, **9**, 270.
3. J. M. Taylor, R. Vaidhyanathan, S. S. Iremonger and G. K. Shimizu, *J. Am. Chem. Soc.*, 2012, **134**, 14338-14340.
4. S. S. Iremonger, J. Liang, R. Vaidhyanathan and G. K. Shimizu, *Chem. Commun.*, 2011, **47**, 4430-4432.
5. S. S. Iremonger, J. Liang, R. Vaidhyanathan, I. Martens, G. K. Shimizu, T. D. Daff, M. Z. Aghaji, S. Yeganegi and T. K. Woo, *J. Am. Chem. Soc.*, 2011, **133**, 20048-20051.
6. B. S. Gelfand, J. B. Lin and G. K. Shimizu, *Inorg. Chem.*, 2015, **54**, 1185-1187.
7. B. S. Gelfand, R. P. S. Huynh, S. P. Collins, T. K. Woo and G. K. H. Shimizu, *Chem. Mater.*, 2017, **29**, 10469-10477.
8. B. S. Gelfand, R. P. Huynh, R. K. Mah and G. K. Shimizu, *Angew. Chem. Int. Ed.*, 2016, **55**, 14614-14617.
9. J. Hynek, P. Brazda, J. Rohlicek, M. G. S. Londesborough and J. Demel, *Angew. Chem. Int. Ed.*, 2018, **57**, 5016-5019.
10. M. Taddei, F. Costantino, A. Ienco, A. Comotti, P. V. Dau and S. M. Cohen, *Chem. Commun.*, 2013, **49**, 1315-1317.
11. M. Taddei, A. Ienco, F. Costantino and A. Guerri, *RSC Adv.*, 2013, **3**, 26177.
12. X. Zhao, J. G. Bell, S.-F. Tang, L. Li and K. M. Thomas, *J. Mater. Chem. A*, 2016, **4**, 1353-1365.
13. S.-F. Tang, X.-B. Pan, X.-X. Lv, S.-H. Yan, X.-R. Xu, L.-J. Li and X.-B. Zhao, *CrystEngComm*, 2013, **15**, 1860.
14. T. Zheng, Z. Yang, D. Gui, Z. Liu, X. Wang, X. Dai, S. Liu, L. Zhang, Y. Gao, L. Chen, D. Sheng, Y. Wang, J. Diwu, J. Wang, R. Zhou, Z. Chai, T. E. Albrecht-Schmitt and S. Wang, *Nat. Comm.*, 2017, **8**, 15369.
15. M. Taddei, F. Costantino and R. Vivani, *Eur. J. Inorg. Chem.*, 2016, **2016**, 4300-4309.
16. G. Yücesan, Y. Zorlu, M. Stricker and J. Beckmann, *Coord. Chem. Rev.*, 2018, **369**, 105-122.
17. A. D. G. Firmino, F. Figueira, J. P. C. Tomé, F. A. A. Paz and J. Rocha, *Coord. Chem. Rev.*, 2018, **355**, 133-149.
18. M. Taddei, F. Costantino, R. Vivani, S. Sabatini, S. H. Lim and S. M. Cohen, *Chem. Commun.*, 2014, **50**, 5737-5740.
19. M. Taddei, F. Costantino, F. Marmottini, A. Comotti, P. Sozzani and R. Vivani, *Chem. Commun.*, 2014, **50**, 14831-14834.
20. N. Hermer, H. Reinsch, P. Mayer and N. Stock, *CrystEngComm*, 2016, **18**, 8147-8150.
21. N. Hermer and N. Stock, *Dalton Trans.*, 2015, **44**, 3720-3723.
22. S. F. Tang, J. J. Cai, L. J. Li, X. X. Lv, C. Wang and X. B. Zhao, *Dalton Trans.*, 2014, **43**, 5970-5973.
23. A. Schütrumpf, A. Bulut, N. Hermer, Y. Zorlu, E. Kirpi, N. Stock, A. Ö. Yazaydın, G. Yücesan and J. Beckmann, *ChemistrySelect*, 2017, **2**, 3035-3038.
24. J. K. Zaręba, *Inorg. Chem. Commun.*, 2017, **86**, 172-186.
25. Y. Zorlu, D. Erbahar, A. Çetinkaya, A. Bulut, T. S. Erkal, O. Yazaydin, J. Beckmann and G. Yücesan, *Chem. Commun.*, 2019, **55**, 3053-3056.
26. T. Rhauderwiek, K. Wolkersdörfer, S. Øien-Ødegaard, K.-P. Lillerud, M. Wark and N. Stock, *Chem. Commun.*, 2018, **54**, 389-392.
27. T. Rhauderwiek, H. Zhao, P. Hirschle, M. Döblinger, B. Bueken, H. Reinsch, D. De Vos, S. Wuttke, U. Kolb and N. Stock, *Chem. Sci.*, 2018, **9**, 5467-5478.
28. B. Wang, T. Rhauderwiek, A. K. Inge, H. Xu, T. Yang, Z. Huang, N. Stock and X. Zou, *Chem. Eur. J.*, 2018, **24**, 17429-17433.
29. G. K. Shimizu, R. Vaidhyanathan and J. M. Taylor, *Chem. Soc. Rev.*, 2009, **38**, 1430-1449.
30. K. J. Gagnon, H. P. Perry and A. Clearfield, *Chem. Rev.*, 2012, **112**, 1034-1054.
31. R. G. Pearson, *J. Am. Chem. Soc.*, 1963, **85**, 3533-3539.
32. T. Devic and C. Serre, *Chem. Soc. Rev.*, 2014, **43**, 6097-6115.
33. T. A. Halgren, *J. Comp Chem.,* 1996, **17**, 490-519.
34. M. D. Hanwell, D. E. Curtis, D. C. Lonie, T. Vandermeersch, E. Zurek and G. R. Hutchison, *J. Cheminformatics*, 2012, **4**, 17.
35. M. Taddei, F. Costantino and R. Vivani, *Inorg. Chem.*, 2010, **49**, 9664-9670.
36. R. Vivani, F. Costantino, U. Costantino and M. Nocchetti, *Inorg. Chem.*, 2006, **45**, 2388-2390.
37. M. Taddei, A. Donnadio, F. Costantino, R. Vivani and M. Casciola, *Inorg. Chem.*, 2013, **52**, 12131-12139.

TABLE OF CONTENTS

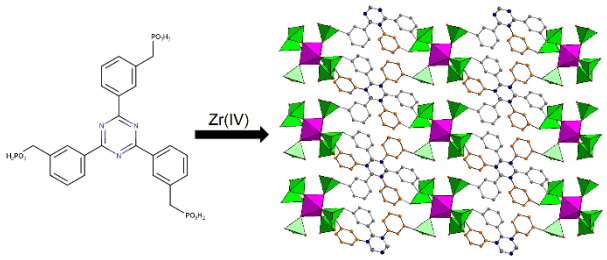

Combination of the novel linker 2,4,6-tris[3-(phosphonomethyl)phenyl]-1,3,5-triazine and Zr(IV) afforded a layered compound that lacks extended inorganic connectivity and displays good proton conductivity.